Adsorption onto Fibrous Activated Carbon: Applications to Water Treatment

ARTICLE *in* ENERGY & FUELS · MARCH 1997

Impact Factor: 2.79 · DOI: 10.1021/ef9601430

Pergamon

Carbon Vol. 35, No. 9, pp. 1307–1313, 1997

0008-6223/97 $17.00 + 0.00

PII: S0008-6223(97)00079-1

ADSORPTION ONTO ACTIVATED CARBON FIBERS: APPLICATION TO WATER AND AIR TREATMENTS

C. BRASQUET and P. LE CLOIREC*
Centre Génie des Procédés de l'Environnement, Ecole des Mines de Nantes, 4 rue Alfred Kastler, BP 20722, 44307 Nantes Cedex 03, France

(*Received* 20 *June* 1996; *accepted in revised form* 31 *March* 1997)

Abstract—The adsorption of polluted fluids is performed by activated carbon fibers (ACF). The adsorption is carried out in batch and in dynamic reactors. Classic models are applied and kinetic constants are computed. Results show that the performance of ACF is significantly higher than that of granular activated carbon (GAC) in terms of adsorption rate and selectivity for micropollutants. The breakthrough curves obtained with ACF adsorbers are particularly steep, suggesting a smaller mass transfer resistance than with GAC. The adsorption zone in the ACF bed is about 3.4 mm and is not really dependent on the water flow rate within the studied range. Applications are developed in water and air treatments. Examples are given in the micropollutants removal of an aqueous solution. Air loaded with VOC is treated by fibers. Regeneration of this material is performed by heating by the Joule effect or electromagnetic induction. These approaches to water or air treatment processes are successfully put to use. © 1997 Elsevier Science Ltd

Key Words—A. Activated carbon, A. carbon fibers, C. adsorption.

1. INTRODUCTION

The removal of organic matter in aqueous or gas phases with granular activated carbon (GAC) is commonly performed for the treatment of water or VOC [1–3]. GAC adsorbers have been proved to be effective in removing a large number of organic molecules [4].

Activated carbon fibers (ACF) have received increasing attention in recent years as an adsorbent for purifying water. The raw materials of ACF are polyacrylonitrile (PAN) fibers, cellulose fibers, phenolic resin fibers or pitch fibers, and cloths or felts made from them. They are first pyrolysed and then activated at a temperature of 700–1000°C in an atmosphere of steam or carbon dioxide [5].

The main objective of the present paper is to assess the performance of the ACF adsorbents in water and air treatments. Phenol and its derivatives are the basic structural units of a wide variety of synthetic organics including many pesticides. Then, aromatics were the model compounds used throughout the adsorption studies in aqueous solutions. The volatile organic compounds (VOC) are well-adsorbed on ACF, an example is shown. Two regeneration methods are briefly described.

2. MATERIALS AND METHODS

2.1 *Activated carbon materials*

Activated carbon materials are commercial products manufactured by the PICA Company and Actitex Company (France). The main characteristics of the materials used in the present investigations are presented in Table 1. The pore size distributions of the two materials are given in Figs 1 and 2. Specific surface areas were determined according to the BET method by helium adsorption. Scanning electronic microscopy pictures of the different adsorbents have been shown elsewhere [6].

2.2 *Water treatment*

2.2.1 *Kinetic and equilibrium studies.* Activated carbon (about 0.6 g) in the form of GAC or ACF was continuously stirred with 1 liter of an aqueous solution at 20 ± 1°C containing initially 100 mg l^{-1} of micropollutants. Samples were withdrawn at regular times and then filtered for analysis until a steady state was obtained, up to 300 minutes for GAC. For the equilibrium studied, the activated carbon mass was varied from 0.05 to 0.5 g in 250 ml of solution. The final solution was then filtered and

Table 1. Main characteristics of activated carbons (PICA Company, Levallois, France, for GAC and Actitex; Levallois, France, for ACF)

	GAC	ACF
Sample identifier	Pica NC 60	Actitex CS 1501
Grain size (mm) or fibrous diameter (μm)	3	10
Precursor	Coconut	Rayon
Porosity	Microporous	Microporous
Specific surface area ($m^2\ g^{-1}$)	1200	1500
Micropore surface area (%)	76.0	87.5
Micropore volume (%)	94.4	96.3
Median pore diameter (Å)	7.3	6.9

*Corresponding author.

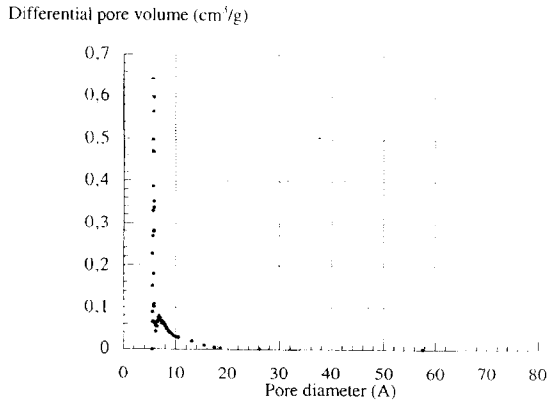

Fig. 1. Pore size distribution of activated carbon fiber CS 1501 (BET method).

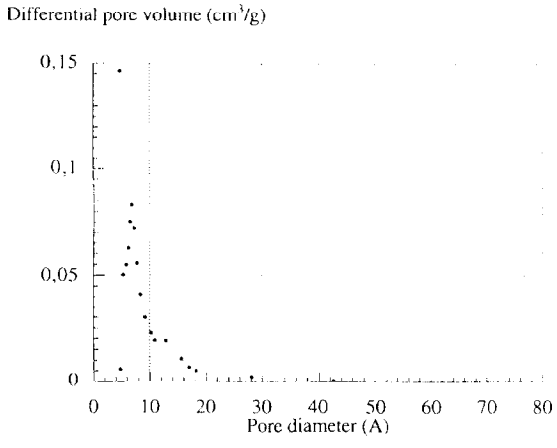

Fig. 2. Pore size distribution of granular activated carbon NC 60 (BET method).

analysed. All reagents were commercially available from the Aldrich Co. Humic substances were extracted from Lake Drumond (U.S.A.) by the Thurman and Malcom method [7–9].

2.2.2 *Adsorption in a continuous flow reactor.* A laboratory pilot unit was set up for the continuous flow study (Fig. 3). The raw water contained 50 mg l^{-1} of micropollutant and was pumped to the adsorption line which was composed of four similar stages, each stage containing 4 mm of ACF. Just one stage is shown in Fig. 3. The modules have a diameter of 2.5 cm. The dead volume inside and between the ACF modules was negligible. The water flowed through each ACF module with a velocity ranging from 0.67 to 2.07 m h^{-1}. Samples were taken at regular times at the outlet of the ACF modules to determine the corresponding breakthrough curves and times.

2.3 *Air treatment*

2.3.1 *Adsorption procedure.* A laboratory pilot unit was set up for the continuous flow study. The raw air contained 50 mg m^{-3} to 50 g m^{-3} of VOC and was sent to the adsorption line. The air velocity through the ACF ranged between 50 and 1000 m h^{-1}. Samples were taken at regular times at the outlet of the ACF modules to determine the corresponding breakthrough times.

2.3.2 *Regeneration.* Two kinds of regeneration were tested. The heating of ACF was developed by the Joule effect (Fig. 4) by means of a 50 Hz generator. The desorption temperature determined the operating conditions (intensity and voltage). Temperatures were measured with thermocouples put on the activated carbon fibers. The experimental procedures have been described elsewhere [10]

The second heating method was developed by electromagnetic induction. Figure 5 shows the activated carbon heating equipment. The column was packed with the activated carbon, with no special pressure applied to the packing material in order to get the same bed porosity for the different experiments. In the specific case of ACF, activated carbon cloth was rolled around an empty cylinder, the adsorbent thickness being about 5 mm. The empty cylinder was put inside a coil. A high frequency generator supplied an oscillatory circuit. The frequency (f) was a function of the number of turns per unit length of the inductor and of the capacitor values (C_i). The temperature measurements were made with thermocouples dispersed in the activated carbon and connected to a Schlumberger Solartron 3430 computer, after the high frequency field has

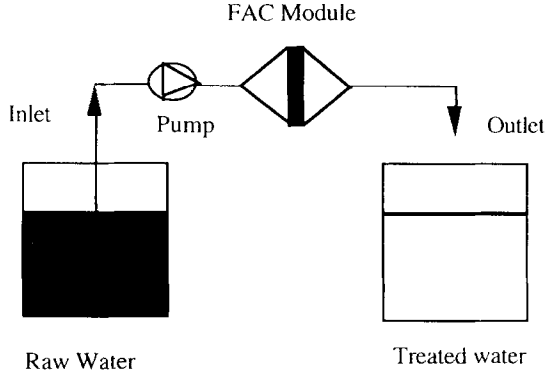

Fig. 3. Continuous flow reactor used in water treatment.

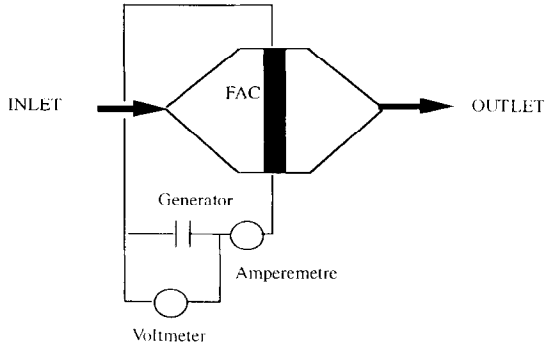

Fig. 4. Heating by the Joule effect: experimental equipment.

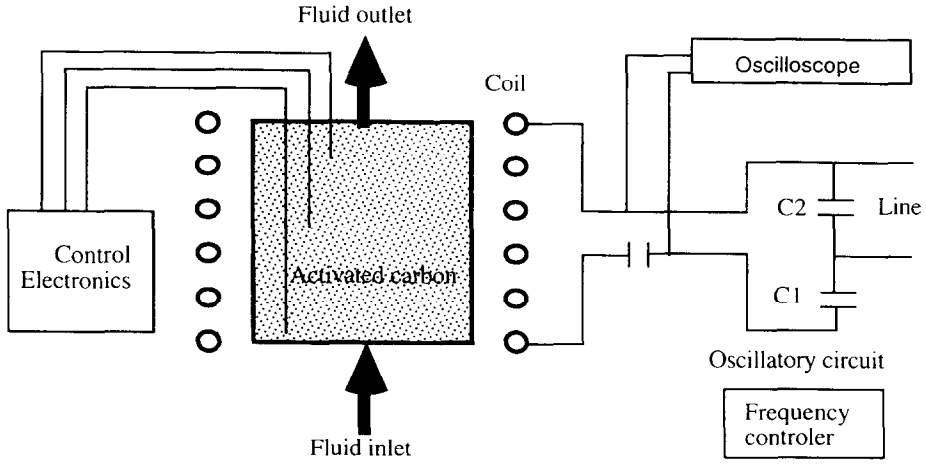

Fig. 5. Experimental equipment used for heating by electromagnetic induction.

been turned off as the field may disturb the operation of the thermocouples [11]. The experimental procedures have been described elsewhere [12].

3. RESULTS AND DISCUSSION

3.1 *Water treatments*

The results are presented in terms of adsorption kinetics, equilibria and selectivity compared to activated carbon granules.

3.1.1 *Adsorption kinetics and equilibria.* The kinetic coefficients were computed for the two activated carbon materials from the initial slopes of the kinetic curves and from the adsorption kinetic data which could be described by the Adam–Bohart–Thomas' relation (eqn (1)):

$$\frac{dq}{dt} = K_1 C(q_m - q) - K_2 q \tag{1}$$

with q: adsorption capacity (mg g^{-1}),
C: solution concentration (mg L^{-1}),
K_1: adsorption kinetic constant (L mg^{-1} s^{-1}),
K_2: desorption kinetic constant (s^{-1}),
q_m: maximal surface concentration (mg g^{-1}),
t: time (s).

At the initial stage of the adsorption reaction, when $t \to 0$, then $q \to 0$ and $C \to C_0$, eqn (1) gives γ, the initial kinetic coefficient:

$$\gamma = -K_1 q_m = -\frac{V}{C_0 m}\left(\frac{dC}{dt}\right)_{t\to 0} \tag{2}$$

with C_0: initial solute concentration in solution (mg L^{-1}),
V: volume of solution (L),
m: mass of the activated carbon in the batch reactor (g).

For organic micropollutants, Freundlich and Langmuir classical models were applied to determine the relation parameters. These models are given by eqns (3) and (4), respectively.

$$q_e = K_e . C_e^{1/n} \tag{3}$$

$$q_e = \frac{b . q_m . C_e}{1 + b . C_e} \tag{4}$$

with q_e: adsorption capacity at equilibrium (mg g^{-1}),
C_e: solution concentration at equilibrium (mg L^{-1}),
K_e: Freundlich's parameter ($mg^{1-1/n}$ $L^{1/n}$ g^{-1}),
$1/n$: Freundlich's parameter,
q_m: maximum adsorption capacity (mg g^{-1}),
b: Langmuir's equilibrium parameter (L mg^{-1}).

Initial kinetic coefficients and Freundlich and Langmuir parameters are shown in Table 2.

Initial adsorption coefficients were higher for ACF than for GAC, with a ratio g_{ACF}/g_{GAC} of about 4. This is due to the fact that ACF micropores are directly on the external surface fiber [6,13,14], and the pore size distribution for PAN-based activated carbon fibers concentrates around 2.5 to 2.6 nm [15]. Thus, adsorbates reach adsorption sites through micropores without additional diffusion resistance of macropores which usually is the rate-controlling step in the case of granular adsorbents [13]. Moreover, the small diameter of the fibers (around 10 μm) results in the large external surface area exposed to the flowing fluid. Thus ACF adsorbents provide much faster adsorption kinetics compared with GAC [10,17].

Furthermore, all isotherms were of type I, demonstrating a favorable adsorption [16]. The Freundlich equilibrium constants were higher for ACF than for GAC probably because of the higher specific surface area and the microporous structure of the activated carbon fibers. On the other hand, Ryu [5] came to the conclusion that the superposition of the adsorption forces generated by the opposite walls of the micropores causes an increase in the adsorption

Table 2. Initial kinetic coefficients, Langmuir and Freundlich model parameters of some aromatic molecules adsorbed onto ACF and GAC (eqns (2)–(4)); na: not adsorbed

Solute	Activated carbon	$\gamma \times 10^5$ (L mg^{-1} min^{-1})	Freundlich			Langmuir		
			$1/n$	K (mg g^{-1})	r	b	q_m (mg g^{-1})	r
Toluene	ACF	7.4	0.182	270.4	0.92	0.07	699.0	0.89
	GAC	2.2	0.204	206.4	0.99	0.344	476.0	0.98
Phenol	ACF	4.8	0.354	56.0	0.96	0.193	208.0	0.92
	GAC	1.9	0.289	50.3	0.99	0.116	184.2	0.98
Benzaldehyde	ACF	7.2	0.276	114.1	0.98	0.557	277.0	0.94
	GAC	2.2	0.278	82.4	0.99	0.217	253.2	0.95
Benzoic acid	ACF	4.6	0.384	82.0	0.99	0.096	422.0	0.97
	GAC	1.4	0.391	53.7	0.97	0.046	371.7	0.97
Humic acid (HA)	ACF	na	na	na	na	na	na	na
Fulvic acid (FA)	ACF	na	na	na	na	na	na	na

potential inside them. Therefore, the ACF materials are more interesting than GAC from the standpoint of adsorption capacities and they were used for the breakthrough experiments.

3.1.2 *Selectivity.* In order to study the selectivity of the two adsorbents, adsorption tests in a batch reactor were performed with a mixture of commercial humic substances and phenol. The results are presented in Fig. 6. Similar isotherm curves were obtained for the two experiments, humic substances being not removed by ACF [18]. The ACF present a selectivity for the low molecular weight molecules (phenol) compared to macromolecules (humic substances). The micropore distribution could explain this selectivity as shown in Fig. 1 and Table 1, the micropore surface area and micropore volume being very high, 87.5 and 96.3%, respectively.

The influence of water on selectivity was studied, and the same experiment was carried out with tap water, deionized water and river water. The results obtained are given in Table 3, they show that the water matrix seems to have little or no influence on the selectivity of ACF for micropollutants in these concentration ranges.

3.1.3 *Dynamic adsorption.* Breakthrough experiments were carried out for the adsorption of phenol onto ACF material with different flow rates through the ACF modules. Typical breakthrough curves for a given flow rate of 2.07 m h^{-1} are presented in Fig. 7. Very steep breakthrough curves were obtained for all the flow rates used in the present investigation. This characteristic shape has already been mentioned in the review by Ryu [5]. Suzuki [13] also showed drastic differences between the breakthrough curves of GAC and packed ACF obtained under the same experimental conditions. The sharper breakthrough curves observed for the ACF suggested smaller mass transfer resistance than for the GAC. Similarly, Ryu [5] concluded that the adsorption rates of ACF are much higher than those of GAC. The breakthrough times were measured when the phenol concentration (C) reached $0.05C_0$ (initial concentration). The values obtained for the various thicknesses and flow rates used in the study

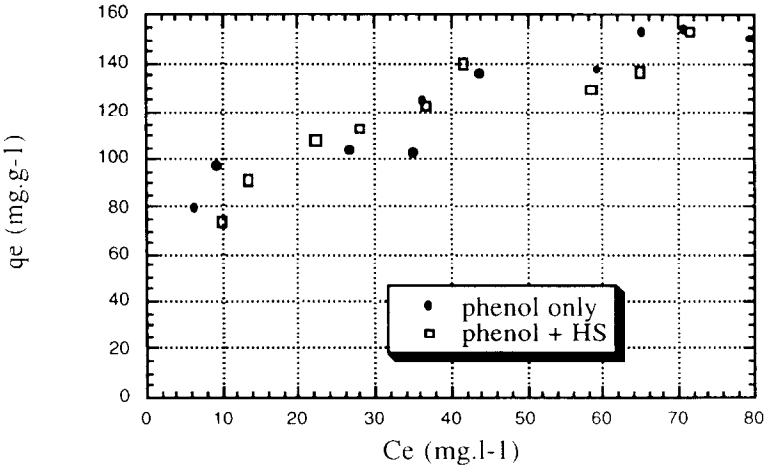

Fig. 6. Adsorption of a mixture of humic substances (HS) and phenol onto ACF.

Table 3. Adsorption capacities (mg g^{-1}) of phenol and humic substances (HS) in different kinds of water

Water	Phenol only	HS only	Phenol in the mixture	HS in the mixture
Deionised	40.1	1	34.3	0
Drinking water	40.3	0.5	32.6	0
River water	44.0	0	40.2	0

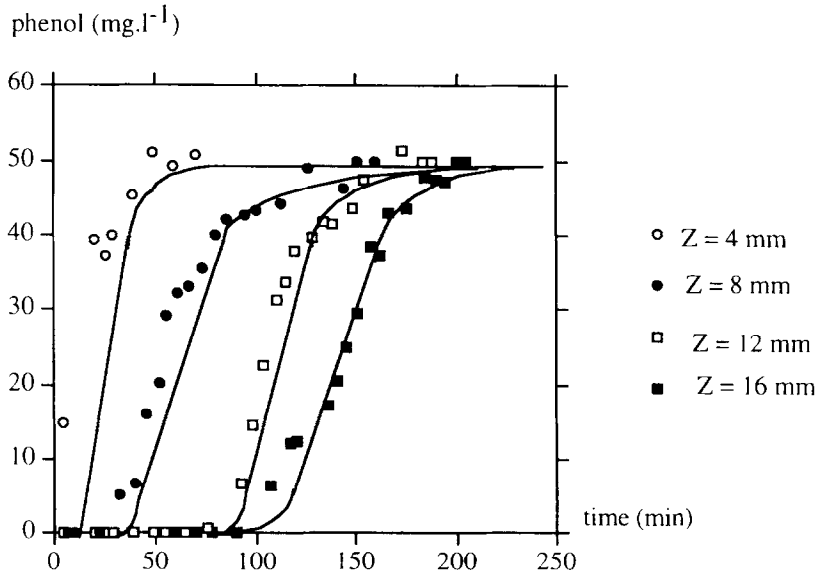

Fig. 7. Breakthrough curves for different thicknesses of ACF (flow rate = 2.07 m h^{-1}; raw water concentration = 50 mg phenol l^{-1}).

were introduced into the bed depth service time (BDST) relation developed by Hutchins [19] and currently used (eqn (5)):

$$t_p = \frac{N_0}{C_0 U_0}(Z - Z_0) \qquad (5)$$

with t_p: breakthrough time (s),
N_0: adsorption capacity (mg l^{-1}),
C_0: initial concentration (mg l^{-1}),
U_0: superficial fluid velocity (m s^{-1}),
Z: thickness of activated carbon bed (m),
Z_0: thickness of mass transfer zone (m).

Parameters of the BDST relation are shown in Table 4. The N_0 (adsorption capacity) and Z_0 (adsorption zone) values were not really strongly dependent on the flow rate within the range 0.62–2.07 m h^{-1}. One might assume that the adsorption process was not significantly influenced by the external mass transfer of the solutes through the hydrodynamic boundary layer. The main resistance to the mass transfer might be due to the diffusion through micropores within the ACF. The adsorption capacities (N_0) were recomputed as a function of the activated carbon weight using the adsorbent bed density (Table 5). A good adsorption capacity (about 130 mg g^{-1}), close to the maximum surface concentrations determined in the batch reactor (Table 2), was found with this dynamic system.

Table 4. Adsorption zone (Z_0) and capacity (N_0) at different flow velocities

U (m h^{-1})	Z_0 (mm)	N_0 (mg l^{-1})	N_0 (m g^{-1})
0.62	3.5	9210	134
1.02	3.3	8925	130
2.07	3.4	8625	126

3.2 *Air treatment*

3.2.1 *VOC adsorption.* A large number of studies were published on the air treatment with activated carbons. Volatile organic compounds (VOC) were found to be well-adsorbed onto GAC

Table 5. Thermal regeneration of ACF by the Joule effect; the regeneration yield is defined as the ratio between the desorbed solvant amount and the adsorbed solvant amount [10]

Experiment number	Electric power (W)	Time to reach 100°C (s)	Regeneration yield (%)
1	240	205	95
2	340	80	100
3	440	55	100

or ACF. During this study, adsorption onto ACF was performed with different VOC. An example is shown in Fig. 8. In this case, the dynamic adsorption capacity was found to be about 30%, i.e. 30 g of solvent per 100 g of ACF. In order to recover the solvent, an "*in situ*" regeneration is required.

3.2.2 *Regeneration of ACF.* Two conventional methods are currently used to desorb VOC from activated carbon by high pressure steam or preheating fluid (air, nitrogen etc.). In order to overcome problems encountered with these conventional methods (polluted condensed steam, high energy consumption, low recovered solvent quality etc.) new processes useful with ACF were considered with the following requirements:

(1) good performances,
(2) no contact between adsorbent and heating source,
(3) high energy density,
(4) lower energy consumption,
(5) safety procedure,
(6) good environmental conditions.

3.2.3 *Regeneration by the Joule effect.* Recently, a thermal regeneration process has been used where the carbon is exposed to a flow of an electric current. The carbon can be either granular [10] or fibrous [20]. The activated carbon structure is akin to a semi-conductor. Laboratory scale experiments on solvent desorption are very promising. The advantage of such a process is that it can be easily implemented *in situ*. Examples of regeneration by the Joule effect on fibrous carbon, loaded with trichloroethylene, are given in Table 6. The time required to reach the desorption temperature is very short. It is obviously a function of the boiling point of the adsorbed solvent, the interaction energies between the solvent and the solid, and the electric power applied on the ACF. In the case of trichloroethylene, a total regeneration is reached, 100% of the adsorbed amount being desorbed by the Joule effect regeneration.

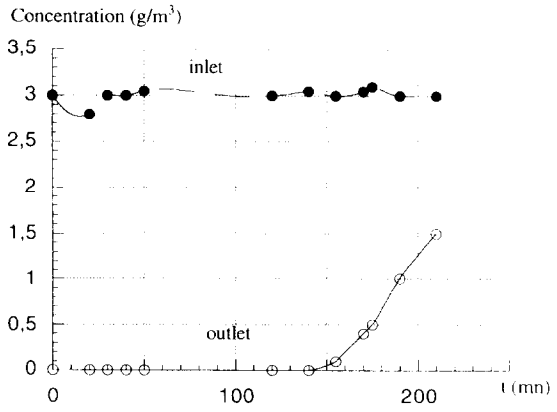

Fig. 8. Breakthrough curve on ACF. Air loaded with perchloroethylene: velocity = 522 m h^{-1}; ACF weight = 7 kg [10].

3.2.4 *Regeneration by induction heating [21–23].* Induction heating can be used to regenerate activated carbon for the purpose of recycling volatile organic compounds. Figure 5 shows the activated carbon heating equipment.

Experiments carried out with ethyl acetate showed that the best frequency ranged from 1 to 100 kHz for the GAC. A regeneration yield of 100% was reached for the granular activated carbon after one hour [12].

As the technological possibilities offered by induction have to be taken into account, the ACF were presented as empty cylinders as described previously. Table 6 gives some preliminary results of heating obtained with ACF. A high temperature is reached very quickly due to the properties of induction heating and mainly to the penetration depth, which is defined by the relation in eqn (6) [24]:

$$\delta = \sqrt{\frac{\rho}{\pi \mu f}} \tag{6}$$

where

δ = penetration depth (m),

ρ = resistivity of carbon ($\Omega \cdot$ m) about $1.64 \times 10^{-3}\ \Omega\ m^{-1}$,

f = current frequency (Hz),

μ = permeability of carbon about 1.24×10^{-3} H m^{-1}.

The penetration depth is computed for different frequencies and the values are between 10 and 4 cm, for $f = 42$ and $f = 263$ kHz, respectively. These data confirm an optimum temperature for the 5 mm thickness activated carbon cloth empty cylinder.

At this time, this kind of regeneration is being developed on a laboratory scale for a treatment by ACF of air loaded by solvents.

4. CONCLUSION

The objective of this study was to determine the efficiency of adsorption of activated carbon fibers in water and air treatments.

Table 6. Preliminary data obtained with induction heating of ACF

Frequency (f) (kHz)	Electric power (Pi) (kW)	Temperature of ACF after 30 seconds (°C)	Penetration depth calculated data (cm)
140	1.1	>120	5
263	1.1	>150	4

Results showed that the ACF provide a high adsorption velocity for aromatic compounds present in water. The kinetic coefficients obtained with the ACF were found between 5 to 10 times greater than those obtained with GAC. Indeed, the microporous structure of fibers and the fact that micropores are directly on the external surface fiber allow a smaller mass transfer resistance.

Classical Langmuir or Freundlich's equations were applied and model parameters were computed. Adsorption capacities were higher with ACF. In the specific case of humic substances, the mainly microporous structure of the ACF prevent the adsorption of this kind of natural organic matter. Furthermore, the treatment of a mixture containing both low and high molecular weight organic compounds showed a similar phenol removal as in the presence of humic substances. These ACF seem to be selective of organic micropollutants.

The breakthrough curves of activated carbon cloths were steep, confirming a small mass transfer resistance. The breakthrough time values obtained for various cloth thicknesses and flow rates were introduced into the bed depth service time (BDST). The N_0 (adsorption capacity) and Z_0 (adsorption zone) values for phenol adsorption were found to be about 130 mg g^{-1} and 3.5 mm, respectively. These parameters were not really strongly dependent of the flow rate within the range 0.62–2.07 m h^{-1}.

ACF also adsorbed VOC well and different regeneration processes were proposed. Preliminary results showed the possibilities of heating ACF by the Joule effect or by electromagnetic induction. A high temperature for solvent desorption was obtained. Regeneration by the Joule effect gave 100% adsorbed solvent recovery in the case of trichloroethylene.

Acknowledgements—The authors thank G. Dagois, Pica Co and E. Subrenat, of the Actitex Co, Levallois, France, for technical assistance, respectively, for the granular activated carbon and fibrous activated carbon used in this study.

REFERENCES

1. Cheremisinoff, P. N. and Ellerbush, M. F., *Carbon Adsorption Handbook*, Ann Arbor Sci, Ann Arbor, MI, 1978.
2. Bansal, R. C., Donnet, J. B. and Stoeckli, N., *Active Carbon*, Marcel Dekker Inc., NY, 1988.
3. Schulhof, P., *J. Am. Water Works Ass.*, 1979, **71,** 648–661.
4. Clark, M. K. and Lykins, B. W., *Granular Activated Carbon*, Lewis Publ., MI, 1989, pp. 257–293.
5. Ryu, S. K., *High Temp.– High Pressures*, 1990, **22,** 345–354.
6. Le Cloirec, P., Baudu, M., Martin, G. and Dagois, G., *Rev. Sci. Tech. Défense*, 1990, **2,** 111–123.
7. Thurman, E. M. and Malcom, R. L., *Environ. Sci. Technol.*, 1981, **15,** 463–466.
8. Christman, R. F., Norwood, D. L., Millington, M. S., Johnson, J. D. and Stevens, A. A., *Environ. Sci. Technol.*, 1983, **17,** 625–628.
9. Le Cloirec, P., Le Lacheur, R. M., Johnson, J. D. and Christman, R. F., *Water Res.*, 1990, **24**(9), 1151–1155.
10. Baudu, M., Le Cloirec, P. and Martin, G., *Environ. Technol.*, 1992, **13,** 423–435.
11. Schlosser, W. J. and Munnings, R. H., *Cryogenics*, 1972, **27,** 1545–1547.
12. Mocho, P., Bourhis, J. C. and Le Cloirec, P., *Carbon*, 1996, **34**(7), 851–856.
13. Suzuki, M., *Water Sci. Technol.*, 1991, **23,** 1649–1658.
14. Abe, M., Kaneko, Y., Agui, W. and Ogino, K., *Sci. Tot. Environ.*, **117/118,** 551–559.1992,
15. Ko, T. S., Chiraniradul, P. and Lin, C. H., *J. Mat. Sci. Letters*, 1992, **11,** 6–8.
16. Weber, W. J. and Smith, E. H., *Environ. Sci. Technol.*, 1987, **21**(11), 1040–1050.
17. Baudu, M., Le Cloirec, P. and Martin, G., *Wat. Sci. Technol.*, 1991, **23,** 1659–1666.
18. Starek, J., Zukal, A. and Rathousky, J., *Carbon*, 1994, **32**(2), 207–211.
19. Hutchins, R., *Chem. Eng.*, 1973, **20,** 133–138.
20. Le Cloirec, P., Baudu, M. and Martin, G., European Patent No. 91460043.2, 1991.
21. Mocho, P. and Le Cloirec, P., in *Studies in Environmental Science 61*, ed. S. Vigneron, J. Hermia and J. Chaouki. Elsevier, Amsterdam, 1994, pp. 251–262.
22. Le Cloirec, P. and Mocho, P., French Patent No. 93 10755, 1993.
23. Bourhis, J. C., Leclerc, O., Le Cloirec, P. and Mocho, P., French Patent No. 95 11466, 1995.
24. Orfeuil, M., *Electrothermie industrielle*, Dunod, Paris, France, 1981.